Appl Phys A (2011) 105:781–788
DOI 10.1007/s00339-011-6667-7

Applied Physics A
Materials Science & Processing

RAPID COMMUNICATION

Thermal transport of oil and polymer composites filled with carbon nanotubes

Vitaliy Datsyuk · Milana Lisunova · Maria Kasimir · Svitlana Trotsenko · Kati Gharagozloo-Hubmann · Izabela Firkowska · Stephanie Reich

Received: 17 October 2011 / Accepted: 25 October 2011 / Published online: 5 November 2011

Abstract We studied the thermal transport properties of multi-walled carbon nanotubes (MWNTs) in polymer and oil matrices. The thermal conductivity of the oils and polymers increased linearly when adding tubes. We observe a particularly high increase in the thermal diffusivity of carbon-nanotube-loaded liquid crystal polymers (6×10^{-5} cm^2/s wt%), which is due to a spontaneous alignment of the MWNTs. Carbon nanotubes increased the thermal conductivity of oil by a factor of three for 20 wt% loading. We found little or no dependence of the thermal enhancement on the specific flavor of multiwall nanotubes used in the composites. Carbon nanotubes are excellent nanoscale fillers for composites in thermal management application.

1 Introduction

Carbon nanotubes (CNT) are well known for their high thermal conductivities [1]. Thermal transport was measured in individual nanotubes by contacting single tubes and small bundles to microfabricated suspended device [2]. The thermal conductivity reached up to 3000 W/mK at room temperature [3], which is higher than the conductivity of diamond under comparable conditions [4]. The experimental results for carbon nanotubes agreed with theoretical predictions [5]. The thermal conductivity of carbon nanotubes measured on bulk samples such as bucky papers, however, is 100 times lower than in individual tubes. In randomly oriented samples the conductivity is on the order of 25 W/mK [6]. An alignment of the nanotubes enhances the thermal conductivity significantly (150–200 W/mK) [7, 8].

Carbon nanotubes are excellent starting materials for application in thermal management. A direct use of nanotubes, e.g., for heat sinks, however, is hindered by the powdery character of macroscopic samples, the likely toxicity of the tubes when airborne, and the high price of the material [9, 10]. A more viable approach is to use nanotubes as thermal fillers in an inexpensive and well manageable matrix material such as polymers, oil, and epoxy resin [11–13].

There is a rich research literature on the synthesis and characterization of nanotube-polymer composites [14–16]. The performance of polymer composites with randomly orientated nanotubes in thermal applications is, generally, quite poor. Room temperature conductivities are on the order of 0.1–1 W/mK for loadings of 1–10 wt% [17, 18]. A notable improvement is achieved upon alignment of carbon nanotubes in the polymer matrix [19, 20], which tends to improve thermal performance by an order of magnitude. Aligned nanotube composites, however, required complicated processing such as in-situ injection molding of CVD-grown nanotubes forests and alignment in porous aluminum oxide [21, 22]. While such materials are important for experimental studies a spontaneous alignment of nanotubes in a polymer matrix is highly desirable for composite preparation.

New types of matrix material for nanotube composites are natural vegetable and fish oils [23]. They are biocompatible and allow the preparation of in-situ polyol composites. Polymers prepared, e.g., from soybean oil are similar in their properties to conventional polymers. Natural oil polymers are promising, environmentally friendly replacements for petroleum-based polymers [24]. Compared to other or-

V. Datsyuk (✉) · M. Lisunova · M. Kasimir · S. Trotsenko · K. Gharagozloo-Hubmann · I. Firkowska · S. Reich
Fachbereich Physik, Freie Universität Berlin, Arnimallee 14, 14195 Berlin, Germany
e-mail: datsyuk@zedat.fu-berlin.de
Fax: +49-30-83856081

ganic compounds natural oils have a high thermal conductivity ($\lambda \approx 0.2$ W/mK) [25]. They may also act as binders for composite samples in thermal management, because the oil reduces the porosity of a sample. Substituting air molecules ($\lambda_{air} = 0.024$ W/mK) in interstitials with the thermally better conducting oil will increase the overall performance of a porous composite.

In this paper we report on the thermal transport properties of nanotube-filled composites with polymers and natural oils as matrix materials. First, we characterize the thermal properties of carbon nanotubes and other nanoscale fillers (nanotubes, graphite, nanodiamond, boron and silicon nitride) after pressing them into macroscopic pellets. The samples have conductivities well below 1 W/mK. The conductivities are much lower than the corresponding bulk values, which is due to the predominance of interfaces in the nanoscale-powder pellets. MWNT-polymer composites yield a linear increase in the thermal diffusivity with wt% nanotube loading. At a given nanotube concentration the relative increase of the diffusivity for cellulose acetate as a matrix was more than three times higher than for PMMA and polyimide. The outperformance of CA results from the partial alignment of carbon nanotubes in this polymer because of its liquid crystal behavior. Adding MWNTs to natural oils yield a strong linear increase in the thermal transport coefficient of the oil. At 10 wt% MWNT loading we observe a doubling of the thermal diffusivity in soybean and olive oil.

This paper is organized as follows. In Sect. 2 we discuss the preparation and characterization of the samples and describe the measurement techniques. Section 3 contains the results of our study combined with a discussion of their implication. In Sect. 4 we summarize our work.

2 Experimental methods

In the present study we use commercially available multi-walled carbon nanotubes. They were industrially produced and purchased from Bayer Materials Science (Baytubes C150P), Nanocyl (NC7000), Fibermax Composites (Fmax MWNT). Figure 1 shows an atomic force microscopy (AFM) image of three batches. The tubes were between 5 and 40 nm in diameter. Typical length was below 10 micron. Selected materials parameters are collected in Table 1. The MWNTs were chemically oxidized with acidic oxidation agents. The samples were refluxed in concentrated nitric acid (HNO_3), as described earlier [26]. To benchmark the MWNT-based nanocomposites we compared the tubes to other nanoscale fillers. Nanodiamonds were supplied by NanoBlox Inc.; boron nitride (BN), silicon carbide (SiC) and silicon nitride (Si_3N_4) nanoparticles were obtained from PlasmaChem. The graphite used in our study is GNP-6 supplied by RMC-Remacon GmbH.

The nanotubes and nanoparticles were pressed in pellets with diameters of 2.54 cm and thickness 0.15–0.18 cm. For

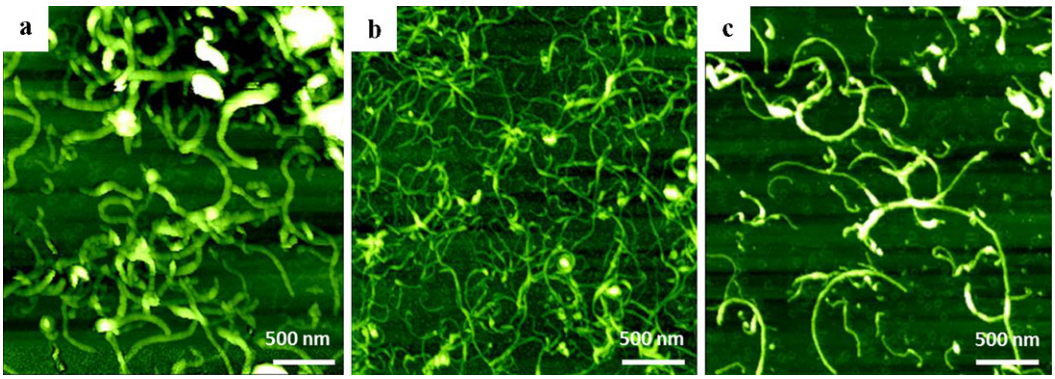

Fig. 1 AFM images of multi-walled carbon nanotubes purchased from (**a**) Bayer Materials Science, (**b**) Nanocyl, and (**c**) Fibermax Composites. Compare also Table 1

Table 1 Main characteristics of CNTs as specified by the supplier

MWNT	Diameter, (nm)	Length, (μm)	Purity, %	Oxygen content, %at.
Baytubes	5–20	1–10	95	0.145
NC7000	9.5	1.5	90	0.391
Fmax MWNT	10–40	1–25	93	0.192

the pressing we used a LaboPress P 200 T (Vogt Maschinenbau GmbH) under pressure force of 200 kN.

For the polymer composites we used cellulose acetate (CA), polymethylmethacrylate (PMMA), and polyimide (PI). All polymers were obtained from Sigma Aldrich. We used two samples of CA with relative molecular mass $M_r = 29{,}000$ and 61,000. The polymers were dissolved in acetone (10 wt%). One batch of polymer solution was used for all composites. As a surfactant we sometimes employed Pluronic® F-68 (polyoxyethylene–polyoxy-propylene–polyoxy-ethylene triblock copolymer, Sigma Aldrich). The matrix materials in the oil composites were soybean, olive oil (Carl Roth GmbH) and fish oil (Vereinigte Fischmehlwerke Cuxhaven GmbH & Co KG).

MWNT-polymer composites were prepared by adding oxidized MWNTs to the polymer solution. This was followed by ultrasonication for 30 min with a Sonopuls HD3100 (Bandelin) equipped with a cup horn operating at 10 kHz and an output power of 100 W. The polymer composites were investigated in liquid (nanofluids) and solid form (composite film). Films were cast onto glass substrate and dried under ambient conditions for 48 hours. These films were than pressed into pellets for the thermal diffusivity measurement. To study the effect of a surfactant on the nanotube-polymer composites we dispersed MWNTs in acetone using Pluronic® F-68 (2 wt%). The dispersion was then added to a polymer solution and treated as described for the MWNT-polymer composites.

Composites of MWNT and natural oil were prepared by adding carbon nanotubes into the oil followed by sonication or mechanical treatment with a three roll mill (Exakt 80E, Exact Advanced Technologies GmbH) with a gap of 15 and 5 μm, respectively. Similar approach was used for preparation of the Graphite-natural oil composites.

We characterized our samples by microscopy. The morphology of MWNT, the polymer and oil composites was examined by scanning electron microscopy (SEM, Hitachi S-4800 with a cold FEG). AFM images were obtained with a Park AFM.

We measured the thermal properties of the starting nanomaterial, the MWNT-polymer and MWNT-oil composites. For the thermal diffusivity measurements we first prepared disks of 25.4 mm in diameter and 5 mm in thickness. They were measured on a XenonFlash XFA500 (Linseis Messgeräte GmbH). The flash method deposits a short, intense energy pulse on one surface of the disk. The pulse was generated by a Xenon lamp with maximum energy pulse of 10 J/pulse. The temperature excursion at the opposite surface is monitored. The characteristic time dependence of the temperature—the thermogram—allows calculating the thermal diffusivity according to the Parker equation [27]

$$\alpha = 0.139 L^2 / t_{1/2}, \tag{1}$$

where L is the sample thickness and $t_{1/2}$ the time for the signal to reach half of its maximum. To measure the diffusivity of liquid oil composites we placed the sample into a stainless steel container with known thermal diffusivity, specific heat, and density of the container material.

From the thermal diffusivity α we calculated the conductivity

$$\lambda = \alpha C_p \rho,$$

where C_p is the specific heat and ρ the density of the material. The specific heat was obtained with a Dynamic Scanning Calorimeter PT1 (Linseis Messgeräte GmbH). We used aluminum crucibles in air atmosphere and a heating rate of 10°C/min. The specific heat was calculated from the heat flux of the composite samples based on the sapphire standard. The bulk density of the samples was calculated as the ratio of sample mass to its volume.

We also measured the thermal conductivity of our samples using a HotDisk Transient Plane Source TPS 2500 S (HotDisk AB). The system uses a nickel wire wound in two intertwined spirals as a sensor. An electrical pulse with a power 0.03–0.5 W in the nickel generates a heat pulse that raises the temperature of the sample [28]. The nickel wire is then used as a sensor to measure the heat dissipation. The HotDisk method requires no special sample preparation. The sensor is simply placed between two pieces of the evaluated materials. All measurements were performed at 23°C.

3 Results and discussion

In this section we present the results of the thermal transport properties of the nanoscale fillers followed by the polymer- and oil-based MWNT composites. The thermal diffusivity measured on pressed pellets of nanoscale fillers are shown in Fig. 2. The thermal diffusivities of the compressed nanomaterials are several orders of magnitude lower than diffusivities of individual nanostructures and bulk samples of the same material.

Pressed powders of nanoscale materials typically show a very poor thermal performance, because thermal transport becomes dominated by the interfaces. We confirm the low coefficients of thermal transport by the independent HotDisk method, see Fig. 3. Similarly low values for the thermal conductivity were reported for powder-pressed samples of unoriented MWNTs (0.15 W/mK in Ref. [29] and 0.25 W/mK in Ref. [30]) and graphite (0.2 W/mK, Ref. [31]). We also note that a Green's function calculation for an unoriented, three-dimensional network of single-walled carbon nanotubes predicted $\lambda = 1$ W/mK [32]. The setting in the calculations—atomically identical, straight, defect-free tubes—certainly serves as an upper bound to our measurements. Pressed pellets of boron nitride nanostructures had

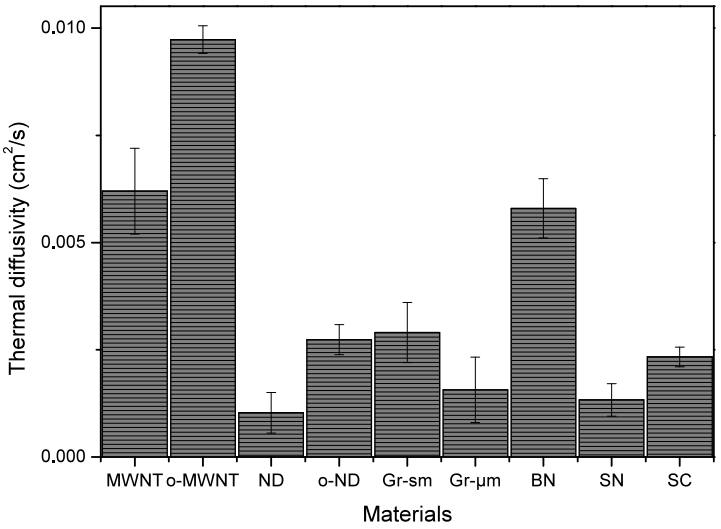

Fig. 2 Thermal diffusivity of nanomaterials measured on compacted pellets. *CNT*: Baytubes, *o-CNT*: oxidized Fmax MWNTs, *ND*: nanodiamonds, *o-ND*: oxidized nanodiamonds, *Gr-sm*: graphite of submicron size, *Gr-µm*: graphite of 200 µm size, *BN*: boron nitride nanoparticles, *SN* (Si_3N_4): silicon nitride nanoparticles, *SC*: silicon carbide nanoparticles

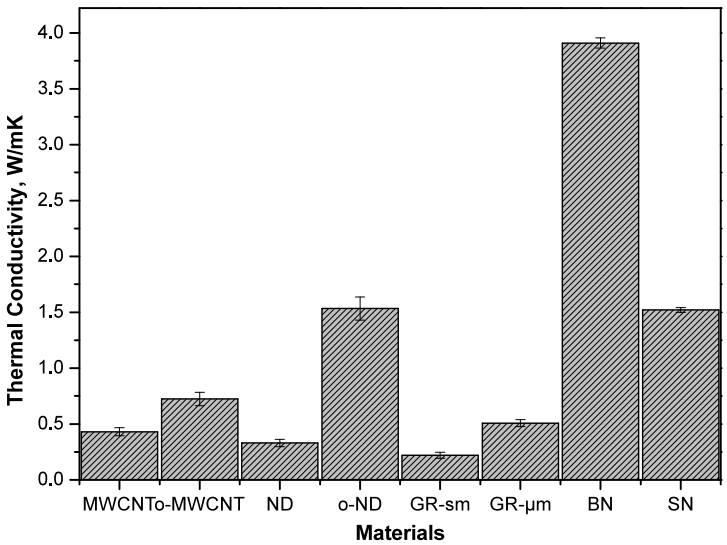

Fig. 3 Thermal conductivity of the nanomaterials measured on compacted pellets by HotDisk

thermal conductivities 0.4–2 W/mK depending on the exact morphology of the nano filler [32]. As for carbon-based materials the powder-pressed pellets of BN nanostructures have a thermal conductivity that is several orders of magnitude lower than in bulk BN (740 W/mK) [33].

Two observations are noteworthy in the thermal diffusivity and conductivity of the powder-pressed samples, see Figs. 2 and 3. First, oxidized nanotubes and nanodiamonds show slightly better thermal performance than the as-received material. This could be due to a better compaction of the oxidized tubes and particles. The measured density of the compacted pellets was 400 and 1300 kg/m^3 for as-received and oxidized MWNTs, respectively. An increase in density generally increases the contact area per link of two nanostructures and hence reduced the interface resistance. Strong increases of the network thermal conductivity with increasing density were reported and observed experimentally [31, 34]. The better packing of the oxidized MWNT can be explained by formation of dense assemblies of nanotubes that bind together through surface groups during solvent drying after oxidation, leading to the reduction of the interfacial resistance [35]. Second, we note the much higher value of the thermal diffusivity for the carbon nanotubes in Fig. 2 compared to the spherical nanodiamonds and graphite. It may arise from the higher aspect ratio of the nanotubes. The observation is in qualitative agreement with the higher thermal conductivity of pellets of cylindrical boron nitride nanotubes (2.2 W/mK) compared to spherical BN particles (0.9 W/mK) [36].

The HotDisk results also confirm the trend of increasing thermal conductivity by oxidation already observed in the diffusivities. The highest thermal conductivity of the boron nitride sample despite their comparatively low thermal diffusivity, Fig. 2, is due to the large specific heat and high density of BN compared to MWNTs [36, 37].

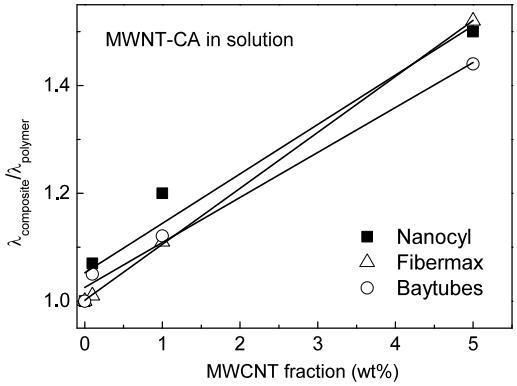

Fig. 4 Thermal conductivity of MWNT-CA-based nanofluids as a function of nanotube contents. *Black squares* are for Nanocyl, open triangle for Fibermax, and *open circles* for Baytubes MWNTs. The *lines* are linear fits to the data points

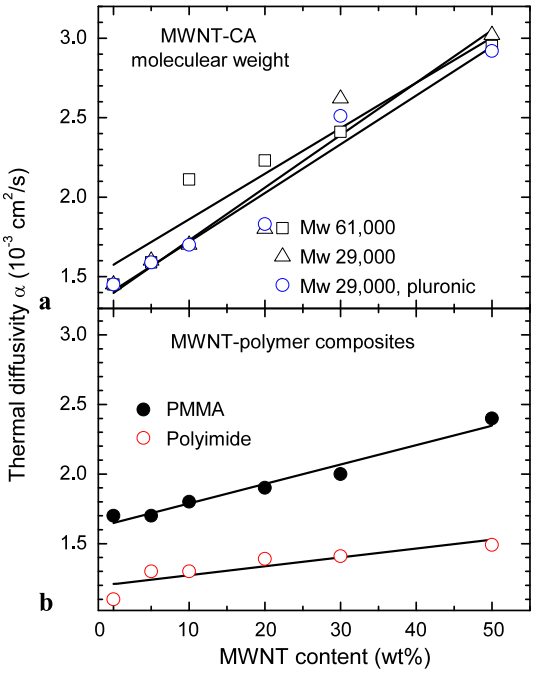

Fig. 5 Thermal diffusivity of the MWNT-polymer composites as a function of MWNT fraction. (**a**) Comparison between the diffusivities for CA with a molecular weight of 61,000 (*squares*) and 29,000 (*triangles*) as well as MWNTs dispersed in CA with 29,000 molecular weight by a surfactant (*circles*). (**b**) Comparison between MWNTs dispersed in PMMA (*closed circles*) and Polyimide (*open circles*)

We now discuss the thermal properties of polymers when embedding carbon nanotubes for increased thermal conductivity. Nanocyl, FiberMax, and Baytubes MWNTs were dispersed in 10 wt% CA solution in acetone. The thermal diffusivity was measured as a function of MWNT content and converted into thermal conductivities, see Fig. 4. There appears to be a linear dependence of the relative thermal conductivity as a function of nanotube loading. The three types of multi-walled nanotube filler result in a similar enhancement of the thermal properties of the CA nanofluids despite the variations in tube diameter. A loading of 5 wt% multi-walled carbon nanotubes into the CA solution leads to an increase of thermal conductivity by a factor of 1.5. Baytubes nanotubes resulted in a slightly lower enhancement (1.4), which could be due to the microsized agglomerates Baytubes are shipped in for safety reasons. The agglomerates require additional mechanical treatment for a homogeneous nanofluid dispersion, which we did not apply here.

The electrical conductivity of most CNT-filled polymer composites varies substantially depending on molecular weight [38]. We evaluated the effect of the polymer chain length on the thermal transport properties and the presence of a surfactant on the composite thermal diffusivity. The thermal diffusivity of MWNT-CA composites with 29,000 and 61,000 CA molecular weight are shown in Fig. 5(a). No significant variation in thermal conductivity of the MWNT-CA composites of the different molecular weight of the matrix polymer was observed. Better MWNT dispersion in the matrix reached with surfactant does not affect the thermal conductivity of the MWNT-CA composites, see Fig. 5(a).

As alternative matrix materials for the dispersion of MWNTs we used polymethyl methacrylate and polyimide resin, Fig. 5(b). Both polyimide resin and PMMA as matrix polymers result in a much lower increase in the thermal conductivity for a given fraction of carbon nanotubes compared to CA. In PMMA composites filled with MWNTs we find a linear increase in the thermal diffusivity of (14 ± 2) cm^2/s. This is more than a factor of two lower than the increase observed for CA. CA and other cellulose derivatives show liquid crystal properties under specific conditions [39]. The liquid crystal behavior leads to an alignment of the MWNT [40], which strongly improves thermal transport in polymer-nanotube networks. We suggest that the higher values of the thermal conductivity in the MWNT-CA composites originate from the MWNT alignment by the cellulose acetate chains. The orientation of the MWNT is also evident in the SEM pictures of the composite as presented in Fig. 6. The figure shows a cross-section of the composite sample where the majority of MWNTs directed perpendicularly to the cut.

For polyimide resin we obtain an increase in the thermal diffusivity of $(6 \pm 2 \times 10^{-3})$ cm^2/s, the lowest value of the composites, see Fig. 4. The combination of polyimide and carbon nanotubes gives rise to a particularly high interface resistance, as we explain now. Polyimide resins are widely used as protective coatings for the metal surfaces [41, 42]. Such coatings show excellent interfacial adhesion, forming a uniform layer on various surfaces [43]. MWNT-polyimide composites have a structure where individual MWNTs or their aggregates are encapsulated in a uniform layer of polyimide. Such an interface is the source of strong phonon scattering and thereby strongly reduces thermal transport.

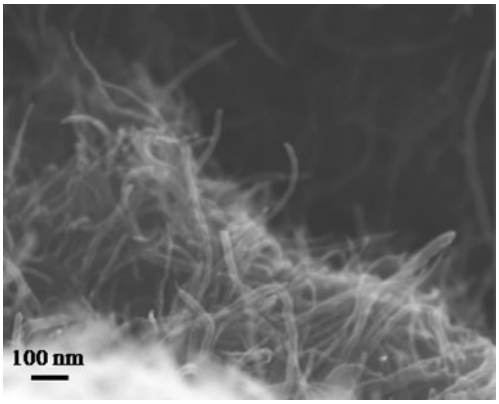

Fig. 6 Scanning electron microscopy image of the MWNT-CA composite with 20 wt% of Baytubes

Newly emerging matrix materials for nanotube thermal composites are natural oils such as plant and fish oils. The thermal diffusivities of MWNTs dispersed in soybean oil are shown in Fig. 7(a). We observe a linear increase in the thermal diffusivity of the oil similar to the MWNT-polymer solution. Fibermax tubes perform better than Baytubes in increasing the thermal diffusivity, which we again attribute to the tendency of Baytubes to form agglomerates. For concentrations of MWNT above 20 wt% the composites become solid. These high-loading composites were pressed into pellets and their thermal diffusivity was measured. The results are presented in Fig. 7(b).

There is a large difference between the extrapolated thermal diffusivity of the fluid samples at 20 wt% (2×10^{-3} cm^2/s) and the measured diffusivity of the solid sample at 20 wt% (4.5×10^{-3} cm^2/s). We think this is caused by the change in measurement setup: The solid samples were measured as pellets with the flash method, whereas the low-concentration liquid samples were placed in a container with known thermal properties, (three-layer method) see Sect. 2. In three-layer method the heat transfer from the bottom and top of the container into the liquid distorts the measurements and might not have been taken into account properly. Nevertheless, both Fig. 7(a) and (b) confirm the linear dependence of the thermal diffusivity on the MWNT concentration; we also obtain a common slope of the Baytube samples (6×10^{-5} cm^2/s wt%) in liquid and solid state.

Samples with MWNT concentration above 40 wt% do no longer form well-compacted pellets or foils. There is an insufficient amount of oil to individualize carbon nanotubes given their high specific surface (ca. 150 m^2/g) [30]. Rather we obtained a MWNT powder wetted with oil. Such samples showed a thermal diffusivity of about 6×10^{-3} cm^2/s. This is in agreement with the value obtained for the compacted raw MWNT, compare Fig. 2. We ascribe the further increase of the thermal diffusivity of the MWNT-oil composite powder is observed due to the perfect substitution of

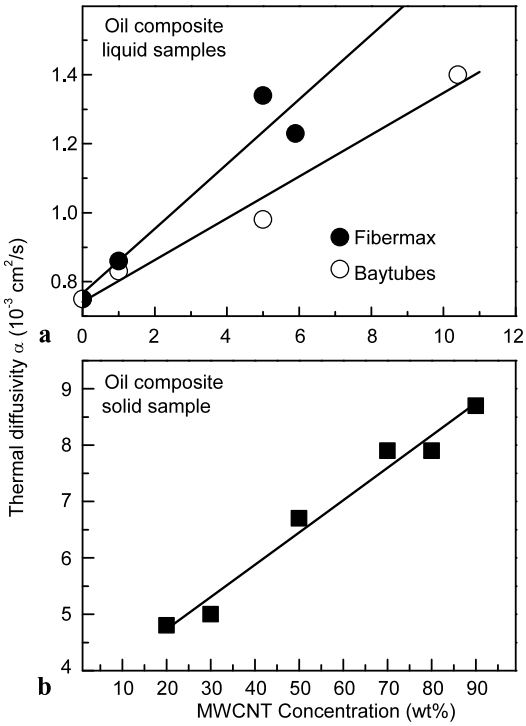

Fig. 7 Thermal diffusivity of MWNT in soybean oil. (**a**) Fibermax (*filled circles*) and Baytubes (*open circles*) MWNTs were dispersed in oil and measured in a container, see Sect. 2. (**b**) Solidified MWNT-oil composites at higher nanotube loading

the air molecules presented in highly porous samples on the oil molecules which have thermal conductivity in one order of magnitude higher compared to air. For highest loading, Fig. 6(b), we were able to reach the thermal diffusivity of oxidized MWNT, Fig. 2, without any chemical treatment.

The influence of the type of nanoscale filler on the thermal conductivity of the composites is presented in Fig. 8. The figure compares the thermal conductivity of MWNTs, graphite and nanodiamonds dispersed in olive oil as measured by the HotDisk technique. The type of filler has a strong influence on the thermal conductivity. The highest improvement in thermal conductivity is achieved by MWNTs with their particularly high aspect ratio. Again Fibermax [slope $(2.2 \pm 0.1) \times 10^{-2}$ W/mK] outperform Baytube nanotubes [$(1.6 \pm 0.1) \times 10^{-2}$ W/mK]. The 40% stronger increase in the thermal conductivity of Fibermax versus Baytubes olive-oil composite is comparable to the 50% steeper increase observed for soybean oil, Fig. 7(a), and the 20% difference for the CA polymer matrix, Fig. 4. Graphite powder dispersed in olive oil considerably enhances the thermal conductivity of the composite. The slope [$(1.4 \pm 0.1) \times 10^{-2}$ W/mK at low loading] is comparable to MWNT. Finally, spherical nanodiamonds only very little increase the composite thermal conductivity, see Fig. 8.

At 25 wt% of MWNT we reached the maximum filler concentration that was dispersible in the olive-oil matrix.

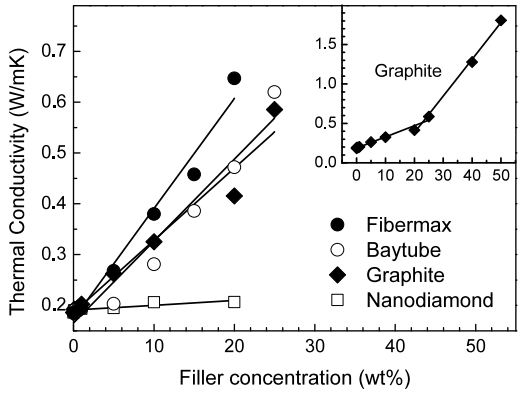

Fig. 8 Thermal conductivity of olive-oil composites filled with Fibermax (*closed circles*) and Baytubes (*opened circles*) MWNTs, graphite (*black diamonds*), and nanodiamonds (*opened squares*). *Lines* are linear fits to the data. The *inset* shows the thermal conductivity of the graphite composites up to a filler concentration of 50 wt%. At high filler concentration the thermal conductivity increases with a three times larger slope than at low filler content as indicated by separate fits above and below 20 wt% loading

For graphite as a filler, however, we achieved much higher filler concentrations, see inset of Fig. 8. Surprisingly, high graphite loading yields a very strong improvement in the thermal transport of the graphite-oil composites. An extrapolation of the linear trend at high loading to pure graphite samples (100% filler concentration) predicts a thermal conductivity of 6 W/mK. This is an order of magnitude larger than the conductivity obtained on pressed graphite pellets, see Fig. 3. A better morphology might partly explain these extremely high conductivities. There might also be an alignment of the graphite particles in the composite.

4 Conclusions

In conclusion, we investigated the thermal transport of carbon nanotubes as raw materials and as nanoscale fillers in polymer and oil composites. A dispersion of nanotubes in composite filler generally leads to a linear increase of the thermal conductivity with increasing content of MWNT. The thermal diffusivity of CA loaded with 50% MWNTs increased by a factor of two; for PMMA and polyimide only 40% increase in the diffusivity was obtained at the same loading. The better performance of CA as a matrix material is due to the alignment of the MWNTs that CA enforces. Natural oils are another promising matrix material for the dispersion of carbon nanotubes. We observe up to tenfold improvement in the thermal diffusivity of soybean oil under extremely high loading of MWNTs. A comparison of oil composites using various nanotubes, graphite and nanodiamond showed that nanoscale fillers with a high aspect ratio yield higher thermal conductivities. Similar trends were observed for pellets of raw nanoscale materials.

Acknowledgements We thank G. Weinberg for help with the SEM. We acknowledge financial support by the BMBF under grant 03F01022.

References

1. J. Hone, M. Whitney, C. Piskoti, A. Zettl, Phys. Rev. B **59**, R2514 (1999)
2. S. Berber, Y.K. Kwon, D. Tománek, Phys. Rev. Lett. **84**, 4613 (2000)
3. J. Hone, M. Whitney, A. Zettle, Synth. Met. **103**, 2498 (1999)
4. D.G. Onn, A. Witek, Y.Z. Qiu, T.R. Anthony, W.F. Banholzer, Phys. Rev. Lett. **68**, 2806 (1992)
5. K. Bi, Y. Chen, J. Yang, Y. Wang, M. Chen, Phys. Lett. A **350**, 150 (2006)
6. P. Gonnet, Z. Liang, E.S. Choi, R.S. Kadambala, C. Zhang, J.S. Brooks, B. Wanga, L. Kramer, Curr. Appl. Phys. **6**, 119 (2006)
7. T. Tong, Z. Yang, L. Delzeit, A. Kashani, M. Meyyappan, A. Majumdar, IEEE Trans. Compon. Packag. Technol. **30**, 92 (2007)
8. D. Wang, P. Song, C. Liu, W. Wu, S. Fan, Nanotechnology **19**, 075609 (2008)
9. A. Helland, P. Wick, A. Koehler, K. Schmid, C. Som, Environ. Health Perspect. **115**, 1125 (2007)
10. A. Carpinteri, N.M. Pugno, J. Phys., Condens. Matter **20**, 474213 (2008)
11. M.J. Biercuk, M. Llaguno, M. Radosavljevic, J.K. Hyun, A.T. Johnson, J.E. Fischer, Appl. Phys. Lett. **80**, 2767 (2002)
12. Y.S. Song, J.R. Yuon, Carbon **43**, 1378 (2005)
13. F.H. Gojny, M.H.G. Wichmann, B. Fiedler, I.A. Kinloch, W. Bauhofer, A.H. Windle, K. Schulte, Polymer **47**, 2036 (2006)
14. J.N. Coleman, U. Khan, W.J. Blau, Y.K. Gun'ko, Carbon **44**, 1624 (2006)
15. A.L. Martínez-Hernández, C. Velasco-Santos, V.M. Castaño, Curr. Nanosci. **6**, 12 (2010)
16. M. Moniruzzaman, K.I. Winey, Macromolecules **39**, 5194 (2006)
17. Y.S. Song, J.R. Youn, Carbon **44**, 710 (2006)
18. P. Bonnet, D. Sireude, B. Garnier, O. Chauvet, Appl. Phys. Lett. **91**, 201910 (2007)
19. B. Pradhan, R.R. Kohlmeyer, J. Chen, Carbon **48**, 217 (2010)
20. H. Huang, C. Liu, Y. Wu, S. Fan, Adv. Mater. **17**, 1652 (2005)
21. Y. Yao, C. Liu, S. Fan, Nanotechnology **17**, 4374 (2006)
22. J.S. Suh, J.S. Lee, Appl. Phys. Lett. **75**, 2047 (1999)
23. T. Braun, L. Mark, R. Ohmacht, U. Sharma, Fuller. Nanotub. Carbon Nanostruct. **15**, 311 (2007)
24. V. Sharma, P.P. Kundu, Prog. Polym. Sci. **31**, 983 (2006)
25. M. Werner, A. Baars, C. Eder, A. Delgado, J. Chem. Eng. Data **53**, 1444 (2008)
26. V. Datsyuk, M. Kalyva, K. Papagelis, J. Parthenios, D. Tasis, A. Siokou, I. Kalitsis, C. Galiotis, Carbon **46**, 833 (2008)
27. W.J. Parker, R.J. Jenkins, C.P. Butler, G.L. Abbott, Appl. Phys. **32**, 1679 (1961)
28. J.A. King, R.A. Hauser, A.M. Tomson, I.M. Wescoat, J.M. Keith, J. Compos. Mater. **42**, 91 (2008)
29. R.S. Prasher, X.J. Hu, Y. Chalopin, N. Mingo, K. Lofgreen, S. Volz, F. Cleri, P. Keblinski, Phys. Rev. Lett. **102**, 105901 (2009)
30. N.R. Pradhan, H. Duan, J. Liang, G.S. Iannacchione, Nanotechnology **20**, 245705 (2009)
31. Y. Chalopin, S. Volz, N. Mingo, J. Appl. Phys. **105**, 084301 (2009)
32. C. Tang, Y. Bando, C. Liu, S. Fan, J. Zhang, X. Ding, D. Golberg, J. Phys. Chem. B **110**, 10354 (2006)
33. G.A. Slack, J. Phys. Chem. Solids **34**, 321 (1973)
34. K. Yang, J. He, P. Puneet, Z. Su, M.J. Skove, J. Gaillard, T.M. Tritt, A.M. Rao, J. Phys., Condens. Matter **22**, 334215 (2010)

35. M.S.P. Shaffer, X. Fan, A.H. Windle, Carbon **36**, 1603 (1998)
36. C. Tang, Y. Bando, C. Liu, S. Fan, J. Zhang, X. Ding, D. Golberg, J. Phys. Chem. B **110**, 10354 (2006)
37. A. Simpson, A.D. Stuckes, J. Phys. C, Solid State Phys. **4**, 1710 (1971)
38. W. Yi, L. Lu, Z. Dian-lin, Z.M. Pan, S.S. Xie, Phys. Rev. B **59**, R9015 (1999)
39. J.N. Coleman, S. Curran, A.B. Dalton, A.P. Davey, B. McCarthy, W. Blau, R.C. Barklie, Phys. Rev. B **58**, R7492 (1998)
40. P. Navard, J.M. Haudin, S. Dayan, P. Sixou, J. Polym. Sci., Polym. Lett. Ed. **19**, 379 (1981)
41. H. Zhang, Z. Wang, Z. Zhang, J. Wu, J. Zhang, J. He, Adv. Mater. **19**, 698 (2007)
42. A.M. Wilson, Thin Solid Films **83**, 145 (1981)
43. E. Watanabe, K. Kanou, T. Kubota, Electrocomp. Sci. Technol. **8**, 15 (1981)